JOURNAL OF CHEMICAL & ENGINEERING DATA

ARTICLE

pubs.acs.org/jced

Kinetic and Equilibrium Studies on Adsorptive Removal of Toluidine Blue by Water-Insoluble Starch Sulfate

Lei Guo,* Guiying Li, Junshen Liu, Songmei Ma, and Jinfeng Zhang

School of Chemistry and Materials Science, Ludong University, Yantai 264025, P. R. China

ABSTRACT: The aim of this research was to estimate the adsorption performance of water-insoluble starch sulfate (SS) for cationic dyes. Toluidine blue (TB), as a model cationic dye, was used to prepare an adsorbate solution. The effects of adsorption time, initial TB concentration, temperature, and initial pH on the adsorption of TB by SS were studied, and the kinetics and equilibrium of the adsorption process were investigated using a nonlinear analysis method. The results showed that SS can effectively remove TB from the aqueous solution. The adsorption kinetic data correlate well with the pseudofirst-order kinetic model. The Langmuir, Freundlich, Toth, and Sips isotherm models were applied in the adsorption equilibrium study. The Toth isotherms had the best applicability to describe the TB adsorption and show that the adsorption energies follow a heterogeneous distribution. The maximum adsorption capacity from the Toth isotherm fitting is 26.56 mg·g^{-1}. The results of thermodynamics studies show that the adsorption process of TB on SS is exothermic in nature. The adsorption of TB on SS is highly pH-dependent, and the optimal adsorption effect is achieved at pH = 6.0.

1. INTRODUCTION

With the development of thet dyeing and finishing industry, dye effluents have become one of the major sources of pollution, especially in China.[1] Because of environmental concerns and significant aesthetic problems, several techniques have been proposed for the removal of dyes from industrial effluents, such as biological treatments,[2] membrane processes,[3] advanced oxidation processes,[4] electrochemical techniques,[5] and adsorption procedures.[6] Among these techniques, adsorption is generally preferred for the removal of dyes from effluents due to its high efficiency, easy handling, and availability of different adsorbents. During the last few decades, studies on adsorption processes focused particular attention on the development of novel and cost-effective adsorbents.[7−10]

Recently, adsorbents based on starch have attracted more and more attention with the aim of developing low-cost and environmentally friendly adsorbents.[11−15] Starch sulfates with a high degree of substitution can be prepared by using sodium bisulfite and sodium nitrite as materials in aqueous solution.[16] Starch sulfates with a high degree of substitution may exhibit good adsorption ability for some substances with a positive charge. However, the excellent swelling properties in aqueous solution make starch sulfates difficult to use as adsorptive materials.

Therefore, the aim of this study was to prepare water-insoluble starch sulfate and study the adsorption process between this modified starch and cationic dyes. Toluidine blue (TB), a cationic thiazine dye, was used as the model cationic dye. The adsorption kinetics and equilibria were thoroughly investigated by using a nonlinear analysis method. The adsorption thermodynamics and the effect of initial pH on the adsorption process were also studied.

2. MATERIALS AND METHODS

2.1. Materials. Corn starch (Zhucheng Xingmao Corn Developing Co., Ltd., food-grade) was dried at 105 °C before it was used. Toluidine blue (TB) (molecular formula, $C_{15}H_{16}ClN_3S$; molecular weight, 305.83; CAS Number, 92-31-9; color index number, 52040; dye content, 85 %; pK_a, 11.8) was obtained from Sinopharm Chemcial Reagent Co., Ltd. and was used without further purification. The chemical structure of TB is shown in Figure 1. Sodium bisulfite, sodium nitrite, and all other commercial chemicals were analytical reagent grade and were used without further purification. All solutions and standards were prepared by using distilled water.

2.2. Preparation of the Adsorbents. Water-insoluble starch sulfates were prepared according to the method described in a previous work.[17] Cross-linked starch was prepared by reacting corn starch with epichlorohydrin, and then water-insoluble starch sulfates were prepared by reacting cross-linked starch with trisulfonated sodium amine ($N(SO_3Na)_3$) according to the method of Cui et al.[16]

A certain amount of sodium bisulfite was dissolved in distilled water in a stirred glass kettle. Then an aqueous solution of sodium nitrite was added dropwise to the kettle at 90 °C and reacted for 1.5 h. In this way, the sulfating agent trisulfonated sodium amine ($N(SO_3Na)_3$) was obtained. After the pH of the sulfating agent solution was adjusted to 9.0, a preweighed amount of cross-linked corn starch was added to this stirred glass kettle. The reaction was allowed to proceed for 4 h at 40 °C. At the end of the reaction time, the product was washed with deionized water three times and then with ethanol only once. The product was then dried at 50 °C in a vacuum for 24 h.

Three samples with different quantities of sulfate groups, named SS1, SS2, and SS3, were prepared to be used as adsorbents. The sulfur content of the adsorbents was determined by elemental analysis (PE 2400II, Perkin-Elmer, USA), and the surface properties

Received: August 30, 2010
Accepted: February 18, 2011
Published: March 09, 2011

dx.doi.org/10.1021/je100891b | J. Chem. Eng. Data 2011, 56, 1875–1881

of the adsorbents were determined by using a surface area and porosity analyzer (ASAP2020, USA). The structures of the adsorbents were analyzed by using a Fourier transform infrared (FTIR) spectrometer (Nicolet Magna IR spectrometer 550, USA).

2.3. Adsorption Experiments. The adsorption experiments were carried out by batch methods. The desired dose of SS was added to 50 mL of aqueous TB solution in a series of 100 mL glass-stoppered Erlenmeyer flasks. The suspension was stirred on a magnetic stirrer at a uniform speed of 120 rpm in a constant temperature bath. After a certain adsorption time, the suspension was filtered through a 0.2 μm nylon membrane by using a syringe filter, and the concentration of TB in the aqueous phase was determined by using a Shimadzu UV−vis spectrophotometer (UV-2550, Japan) at the maximum wavelength of 630 nm. The initial pH value of the TB solution was adjusted by adding either 0.1 M HCl solution or 0.1 M NaOH solution before adding the adsorbent. Triplicate experiments were made for each condition.

The adsorption capacity was calculated from the following expression:

$$Q = \frac{(C_i - C_t)V}{m} \quad (1)$$

where Q is the adsorption capacity of the adsorbent ($mg \cdot g^{-1}$), C_i and C_t ($mg \cdot L^{-1}$) are the initial and terminal concentrations of TB in the adsorption solution, respectively, and V (L) and m (g) are the volume of the adsorption solution and the dose of the adsorbent, respectively.

3. RESULTS AND DISCUSSION

3.1. Characterization of Adsorbents. Elemental analysis results of the adsorbents are shown in Table 1. The sulfur content of the adsorbents is in the order of SS1 < SS2 < SS3, which means the content of active sulfate groups changes in the same order. The surface properties of the adsorbents were determined by using a surface area and porosity analyzer, and the results are shown in the Table 2. The data of the surface properties have no direct relation to the sulfur content of the adsorbents. The IR spectra of the native corn starch, cross-linked starch, and SS1 are shown in Figure 2. There is no significant difference in the IR spectra between the native starch and the cross-linked starch. Bands resulting from S═O stretching at 1238 cm^{-1} and from S−O stretching at

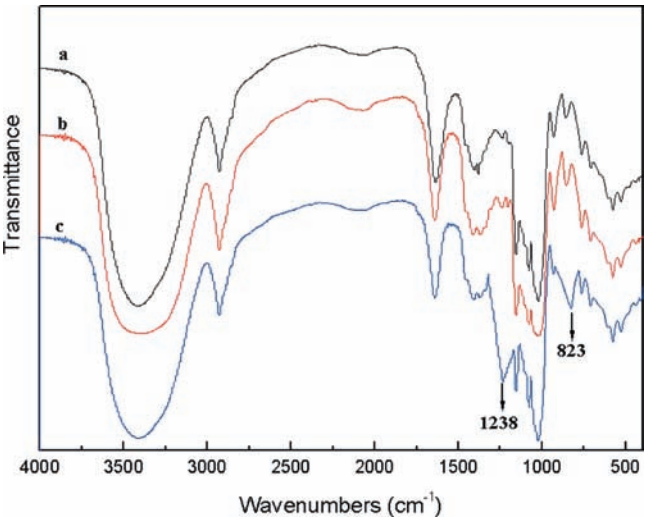

Figure 2. IR spectra of native starch (a), cross-linked starch (b), and SS1 (c).

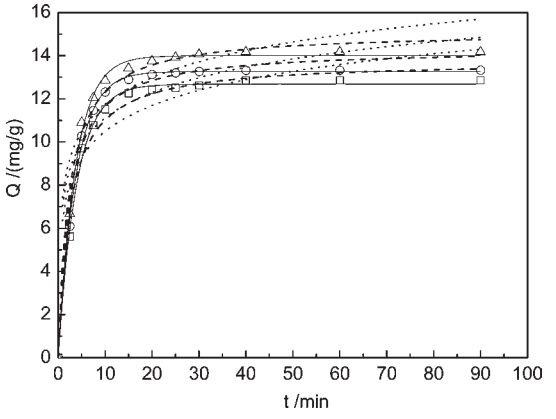

Figure 3. Effect of the adsorption time on the adsorption capacities of TB and the kinetic fitting curves (Conditions: C_i, 16 $mg \cdot L^{-1}$; temperature, 293 K; dose of SS, 50 mg; pH, 5.24): □, SS1; ○, SS2; △, SS3; —, pseudofirst-order; - - -, pseudosecond-order; · · ·, Elovich.

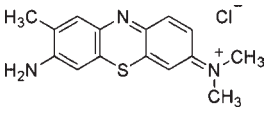

Figure 1. Chemical structure of toluidine blue (λ_{max} = 630.0 nm).

Table 1. Elemental Analysis Results of SS

samples	found (%)				
	C	H	N	S	O
SS1	29.71	4.15	0.37	13.09	52.68
SS2	27.05	3.71	0.36	15.58	53.3
SS3	23.31	3.21	0.39	18.82	54.27

Table 2. Surface Area and Pore Parameters for SS

parameters	SS1	SS2	SS3
surface area			
single point surface area at p/p^0 = 0.20/($m^2 \cdot g^{-1}$)	0.31	0.40	0.32
BET surface area/($m^2 \cdot g^{-1}$)	0.42	0.25	0.35
pore volume			
BJH adsorption cumulative volume of pores between 1.7000 and 300.0000 nm diameter/($10^3 \cdot cm^3 \cdot g^{-1}$)	0.65	0.58	0.71
pore size			
adsorption average pore width (4 V/A by BJH)/(nm)	7.58	5.61	7.32

dx.doi.org/10.1021/je100891b |J. Chem. Eng. Data 2011, 56, 1875–1881

823 cm^{-1} can be observed in the spectrum of SS1, which are similar to the result of Cui et al.[16] These two bands can prove that the product is starch sulfate.

3.2. Adsorption Kinetics Studies. Adsorption kinetics involves the relationship between the adsorption capacities and adsorption time. The adsorption capacities of toluidine blue (TB) on water-insoluble starch sulfate (SS) were measured as a function of time, as shown in Figure 3. TB is rapidly removed by SS and the adsorption processes reach equilibrium in about 40 min. Although the quantity of active sulfate groups was different the equilibrium time was almost the same. Figure 3 also shows the adsorption capacity of TB increases with an increase in the content of sulfate groups in the three sulfated samples. This phenomenon can be explained by the adsorption mechanism between TB and SS, as can be shown in Figure 4. The adsorption of TB on other adsorbents was also rapid due to its cationic character. Sheng et al.[18] studied the adsorption of TB on extracellular polymeric substances extracted from sludge and found that the adsorption equilibrium time was 30 min at pH 11.0. Alpat et al.[19] studied the adsorption kinetics of TB with Turkish zeolite and found that the equilibrium time was also 30 min.

The adsorption kinetics in wastewater treatment is important, as they provide valuable insights into adsorption system design. A variety of kinetic models have been described in an attempt to find a suitable mechanistic explanation for solid/liquid adsorption systems, in which Lagergren's pseudofirst-order,[20] Ho's pseudosecond-order[21] and the Elovich models[22] are the three most widely applied. The forms of the three kinetic models are summarized in Table 3 and were used to correlate the present experimental data. In the kinetic equations, Q_t ($mg \cdot g^{-1}$) is the adsorption capacity at any time t (min).

The nonlinear regression analysis method was used to fit the kinetic models as well as the isotherm models with the help of the Origin (Version 8) software program. Recent studies have shown that the nonlinear method is more valid than the linear method for fitting either the kinetics model[23] or isotherm models.[24]

The nonlinear fitting curves of the pseudofirst-order, pseudosecond-order, and Elovich equations for adsorption of TB on SS are presented in Figure 3. The kinetic model parameters are shown in Table 4 along with the coefficients of determination (R^2). The values of R^2 indicate that the best fit is with the pseudofirst-order model. The Elovich model is not fully followed in this process due to much lower values of R^2. In many other cases, the pseudofirst-order kinetic model provided better results for the adsorption of dyes from aqueous solution by using bioresource adsorbents.[9,25]

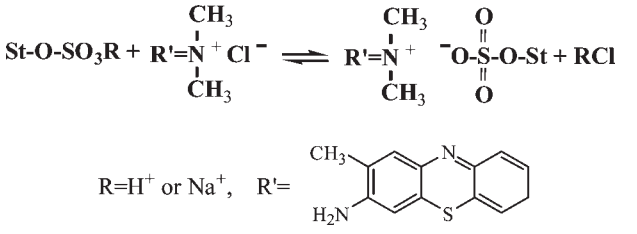

Figure 4. Scheme of the adsorption mechanism between TB and SS.

3.3. Adsorption Equilibrium Studies. The effect of initial TB concentration on the equilibrium adsorption capacity was studied, and the results are shown in Figure 5A. It can be seen that the equilibrium adsorption capacity of TB on SS increases with a rise in the initial TB concentration. When the initial TB concentration is increased from 4.00 $mg \cdot L^{-1}$ up to 32.00 $mg \cdot L^{-1}$, the adsorption capacities of SS1, SS2, and SS3 increase from (3.40 to 22.56) $mg \cdot g^{-1}$, (3.51 to 23.83) $mg \cdot g^{-1}$, and (3.57 to 25.75) $mg \cdot g^{-1}$, respectively. The increase in adsorption capacity with respect to the TB concentration is probably due to a high driving force for mass transfer.

The equilibrium adsorption isotherms express the specific relation between the concentration of adsorbate and its degree of accumulation onto the adsorbent surface at equilibrium. The Langmuir[26] and Freundlich models,[27] the two two-parameter adsorption isotherm models, are widely used to describe the equilibrium of an adsorption process between the liquid and the solid phases. The Sips[28] and Toth models[29] are three-parameter isotherm models, which may provide more information on the adsorption process than two-parameter isotherm models. The four isotherm models are summarized in Table 5 and have been applied in the present study. In the four equations, C_e and Q_e are

Table 4. Kinetic Model Parameters for the Adsorption of TB on SS (Conditions: C_i, 16 $mg \cdot L^{-1}$; Temperature, 293 K; Dose of SS, 50 mg; pH, 5.24)

		sample		
kinetic models	parameters	SS1	SS2	SS3
pseudofirst-order	$Q_e/(mg \cdot g^{-1})$	12.68	13.26	13.99
	$K_1/(min^{-1})$	0.256	0.268	0.272
	R^2	0.9961	0.9977	0.9969
pseudosecond-order	$Q_e/(mg \cdot g^{-1})$	13.76	14.32	15.11
	$K_2/[g \cdot (mg \cdot min)^{-1}]$	0.029	0.030	0.029
	R^2	0.9823	0.9795	0.9854
Elovich	$\alpha/[mg \cdot (g \cdot min)^{-1}]$	74.48	117.22	123.80
	$\beta/(g \cdot mg^{-1})$	0.58	0.59	0.56
	R^2	0.9259	0.9197	0.9322

Table 3. Summary of Adsorption Kinetic Models Used in the Present Study

kinetic models	parameters	ref
pseudofirst-order $Q_t = Q_e(1 - e^{-K_1 t})$ (2)	K_1: the pseudofirst-order rate constant (min^{-1}); Q_e: the equilibrium adsorption capacity ($mg \cdot g^{-1}$)	20
pseudosecond-order $Q_t = \frac{K_2 Q_e^2 t}{1 + K_2 Q_e t}$ (3)	K_2: the pseudosecond-order rate constant [$g \cdot (mg \cdot min)^{-1}$]; Q_e: the equilibrium adsorption capacity ($mg \cdot g^{-1}$)	21
Elovich $Q_t = \frac{1}{\beta}\ln(\alpha\beta) + \frac{1}{\beta}\ln t$ (4)	α: the Elovich coefficient representing the initial adsorption rate [$mg \cdot (g \cdot min)^{-1}$]; β: the Elovich coefficient related to the extent of surface coverage and activation energy for chemisorption ($g \cdot mg^{-1}$)	22

dx.doi.org/10.1021/je100891b |J. Chem. Eng. Data 2011, 56, 1875–1881

the equilibrium TB concentration ($mg \cdot L^{-1}$) and equilibrium adsorption capacity ($mg \cdot g^{-1}$), respectively; Q_m is the constant representing maximum adsorption capacity ($mg \cdot g^{-1}$).

The effect of the equilibrium TB concentration on the adsorption capacities and adsorption equilibrium isotherms is shown in Figure 5B. The best model could be selected on the basis of the values of R^2. It is clear from Figure 5B and Table 6 that the three-parameter isotherm models represent the experimental data better than the two-parameter isotherm models. A further comparison of the values of R^2 from the two-parameter isotherm models fitting shows the Langmuir model provides a better fit of the data than the Freundlich model. Between the two three-parameter isotherm models, the Toth model correlates the data better than the Sips model. Considering all the above results, the equilibrium data of TB adsorption on all three samples can be described in the order of fitting: the Toth, Sips, Langmuir, and Freundlich isotherm models.

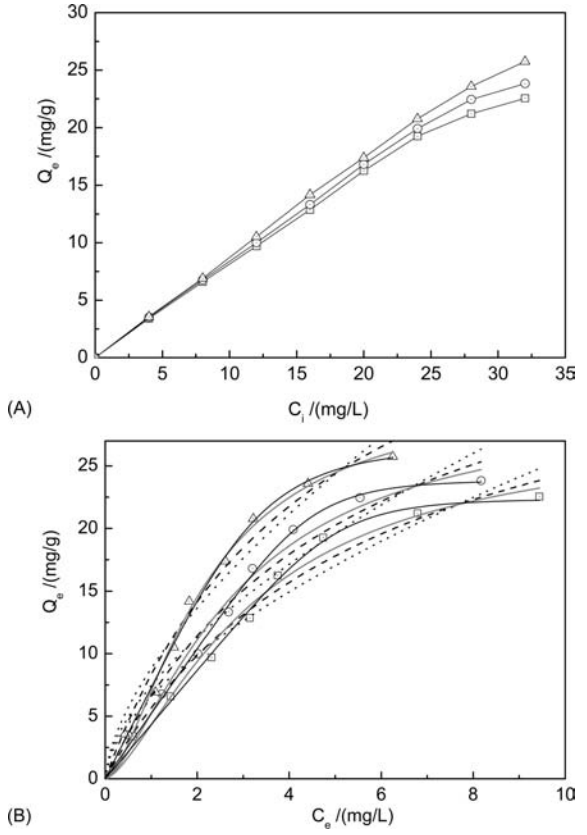

Figure 5. Effect of the (A) initial and (B) equilibrium TB concentration on the adsorption capacities and adsorption equilibrium isotherms (Conditions: adsorption time, 60 min; temperature, 293 K; dose of SS, 50 mg; pH, 5.24): (A): —□—, SS1; —○—, SS2; —△—, SS3. (B): □, SS1; ○, SS2; △, SS3; - - -, Langmuir; · · ·, Freundlich; gray —, Sips; black —, Toth.

The Toth model is derived from potential theory and is applicable to heterogeneous adsorption. It assumes a quasi-Gaussian energy distribution. The more the parameter t is away from unity, the more heterogeneous is the system. The best applicability of the Toth isotherms to the TB adsorption shows that the mechanism of adsorption follows a heterogeneous distribution of adsorption energies. A possible reason is that all three amidocyanogens of TB (Figure 1) have the possibility to consist of valence forces with the sulfate groups on the adsorbents. This means that two or three amidocyanogens of some TB molecules come into covalent bonding proximity of the sulfate groups at the same time. Obviously, the adsorption energies between different amidocyanogens and the sulfate groups are different. Another possible reason is the interactions between TB molecules. TB molecules possibly form dimers and aggregates on the external surface of the adsorbents.[30,31]

3.4. Adsorption Thermodynamic Studies. The thermodynamics for the adsorption of TB on water-insoluble starch sulfate

Table 6. Isotherm Model Parameters for the Adsorption of TB on SS (Conditions: Adsorption Time, 60 min; Temperature, 293 K; Dose of SS, 50 mg; pH, 5.24)

		sample		
isotherms	parameters	SS1	SS2	SS3
Langmuir	$Q_m/(mg \cdot g^{-1})$	38.50	41.90	47.13
	$K_L/(L \cdot mg^{-1})$	0.17	0.19	0.21
	R^2	0.9812	0.9804	0.9848
Freundlich	$K_F/[(mg \cdot g^{-1})(mg \cdot L^{-1})^{-1/n}]$	6.59	7.45	8.81
	$1/n$	1.69	1.66	1.58
	R^2	0.9577	0.9575	0.9642
Sips	$Q_m/(mg \cdot g^{-1})$	27.87	29.87	30.96
	$K_S/(L \cdot mg^{-1})$	0.32	0.35	0.46
	s	0.68	0.67	0.63
	R^2	0.9887	0.9882	0.9940
Toth	$Q_m/(mg \cdot g^{-1})$	22.36	23.86	26.56
	K_T	0.19	0.22	0.28
	t	5.94	5.75	3.67
	R^2	0.9968	0.9972	0.9958

Table 5. Summary of Adsorption Isotherms Used in the Present Study

isotherm	equation		parameters	ref
Langmuir	$Q_e = \frac{Q_m C_e}{1 + K_L C_e}$	(5)	K_L: the Langmuir equilibrium constant related to adsorption affinity, $L \cdot mg^{-1}$	26
Freundlich	$Q_e = K_F C_e^{1/n}$	(6)	K_F: the Freundlich constant related to the adsorption capacity, $(mg \cdot g^{-1})(mg \cdot L^{-1})^{-1/n}$; n, the Freundlich constant related to adsorption intensity	27
Sips	$Q_e = \frac{Q_m (K_S C_e)^{1/s}}{1 + (K_S C_e)^{1/s}}$	(7)	K_S: the Sips equilibrium constant related to adsorption affinity, $L \cdot mg^{-1}$; s: the heterogeneity factor	28
Toth	$Q_e = \frac{Q_m K_T C_e}{[1 + (K_T C_e)^t]^{1/t}}$	(8)	K_T: the Toth constant characterizing the adsorptive potential; t: constant characterizing the heterogeneity	29

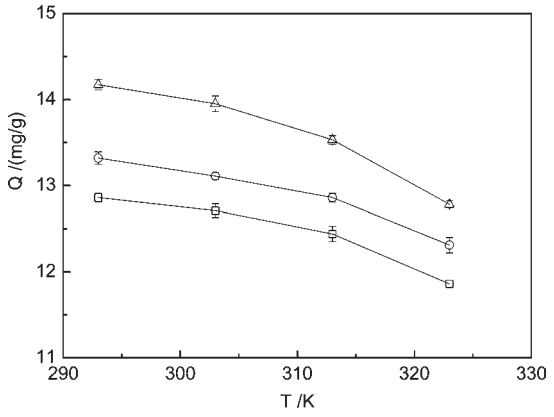

Figure 6. Effect of the temperature on the adsorption capacity for TB on SS (Conditions: C_i, 16 mg·L^{-1}; adsorption time, 60 min; dose of SS, 50 mg; pH, 5.24): —□—, SS1; —○—, SS2; —△—, SS3.

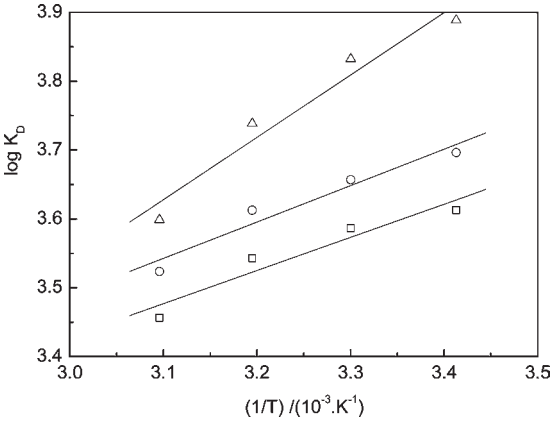

Figure 7. Plots of log K_D versus $1/T$ for the adsorption of TB on SS (Conditions: C_i, 16 mg·L^{-1}; adsorption time, 60 min; dose of SS, 50 mg; pH, 5.24): □, SS1; ○, SS2; △, SS3.

was investigated in the range of (293 to 323) K, and the influence of temperature on the adsorption is shown in Figure 6. It can be found that there is a slight decrease for the equilibrium adsorption capacity with a temperature increase from (293 to 323) K.

Thermodynamic parameters such as change in Gibbs energy (ΔG), enthalpy (ΔH), and entropy (ΔS) were determined using the following equations:[32,33]

$$K_D = \frac{Q_e}{C_e \cdot 10^{-3}} \quad (9)$$

$$\log K_D = -\frac{\Delta H}{2.303RT} + \frac{\Delta S}{2.303R} \quad (10)$$

$$\Delta G = \Delta H - T\Delta S \quad (11)$$

where K_D ($10^3 \cdot L \cdot g^{-1}$) is the distribution coefficient, and K_D can be regarded as a dimensionless coefficient in dilute aqueous solutions; Q_e (mg·g^{-1}) and C_e (mg·L^{-1}) are the adsorption capacity and TB concentration at equilibrium, respectively, T is the temperature in Kelvin and R is the gas constant. ΔH and ΔS were obtained from the slope and intercept of the plots of log K_D versus $1/T$ (Figure 7). Table 7 shows the calculated values of the thermodynamic parameters. The values of ΔG become less

Table 7. Thermodynamic Parameters for the Adsorption of TB on SS (Conditions: C_i, 16 mg·L^{-1}; Adsorption Time, 60 min; Dose of SS, 50 mg; pH, 5.24)

	T	Q_e	K_D	ΔG	ΔH	ΔS
sample	K	mg·g^{-1}	10^3·L·g^{-1}	kJ·mol^{-1}	kJ·mol^{-1}	J·(mol·K)$^{-1}$
SS1	293	12.86	4.10	−20.35	−9.22	37.99
	303	12.71	3.86	−20.73		
	313	12.44	3.49	−21.11		
	323	11.86	2.86	−21.49		
SS2	293	13.32	4.97	−20.8	−10.12	36.45
	303	13.11	4.54	−21.16		
	313	12.86	4.10	−21.53		
	323	12.31	3.34	−21.89		
SS3	293	14.17	7.74	−21.94	−17.35	15.67
	303	13.95	6.80	−22.1		
	313	13.53	5.48	−22.25		
	323	12.78	3.97	−22.41		

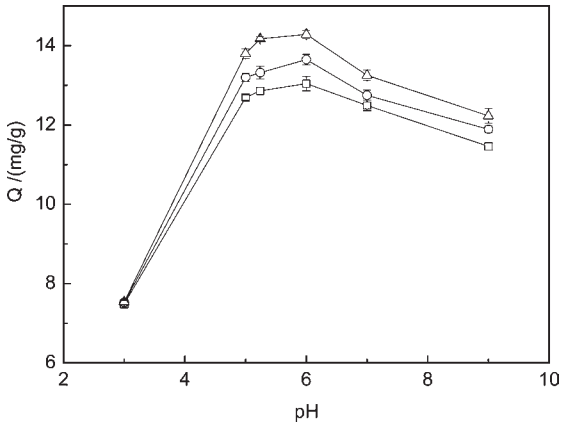

Figure 8. Effect of initial pH on the adsorption capacities of TB on SS (Conditions: C_i, 16 mg·L^{-1}; adsorption time, 60 min; temperature, 293 K; dose of SS, 50 mg): —□—, SS1; —○—, SS2; —△—, SS3.

negative with increasing temperature, and all of the values of ΔH are negative, which indicate that the adsorption process is more favorable at low temperature. Similar results were found in the studies of Şener[34] and Demir et al.[35] The positive values of ΔS indicate that there is an increase in the randomness in the solid−solution interface during the adsorption process. In addition, the small values of ΔG and ΔH are in the range of multilayer adsorption and are compatible with the formation of weak chemical interactions between sulfate groups and TB.[36,37] The complicated interaction between TB and SS has been explained in the equilibrium studies part.

3.5. Effect of Initial pH on the Adsorption Process. The value of pH is one of the most important factors that affect the adsorption process. Figure 8 shows the effect of pH on the adsorption of TB on SS in the initial pH ranges of 3.0 to 9.0. As the pH values increase from 3 to 6, the adsorption capacities of TB increase gradually and reach a maximum value at about pH 6. Then the adsorption capacities decrease gradually with the pH increasing from 6 to 9. The effect of pH on the adsorption process can be explained with the protonation of the functional

Table 8. Previously Reported Adsorption Capacities and Time to Reach Equilibrium for Various Adsorbents for TB Adsorptions

	Q_m	time	
adsorbents	$mg \cdot g^{-1}$	min	ref
Turkish zeolite	33.03	30	19
fly ash	6	--	31
gypsum	28	60	39
pulp fiber	25	240	40
SS3	47.13	40	present study

groups on the adsorbents as well as adsorbates. At low pH values, the high concentration of the H^+ in solution makes the sulfate groups exist in the form of $-SO_3H$, and they prevent the adsorption of TB onto SS. This implies that the active groups are protonated. At pH 6.0, the active sites become ionized, and the cationic TB becomes adsorbed due to better valence forces between TB and SS. When the pH values increase beyond 6.0, the amidocyanogens of TB become less positive, and therefore the adsorption capacities decrease. Similar findings were reported for the adsorption of malachite green on oil palm trunk fiber[9] and rhodamine B on sodium montmorillonite.[38]

3.6. Comparison with Other Adsorbents. To justify the validity of insoluble starch sulfate as an adsorbent of TB, the maximum adsorption capacity and the time to reach equilibrium for the adsorption of TB on SS3 and other various adsorbents are compared in Table 8. The maximum adsorption capacity is from the Langmuir isotherm, and the time to reach equilibrium is estimated from the effect of adsorption time on the adsorption capacities. It shows that SS3 has good adsorption capacity and a relatively short adsorption time when compared with other adsorbents.

4. CONCLUSIONS

The adsorption of toluidine blue (TB) on water-insoluble starch sulfates (SS) from aqueous solution has been thoroughly studied. On the basis of kinetic experimental data, the adsorption processes reach equilibrium in about 40 min and conform to the pseudofirst-order model. The results of adsorption equilibrium studies show that the Toth equation represents the best fit of experimental data among the Langmuir, Freundlich, Toth, and Sips isotherm models. The maximum adsorption capacity of SS3 from the Toth isotherm fitting is 26.56 $mg \cdot g^{-1}$. The best applicability of the Toth isotherms means the adsorption of TB on SS is heterogeneous. All of the values of ΔH are negative, which indicates that the adsorption process is exothermic in nature. Adsorption thermodynamic studies reveal the adsorption mechanism via weak ionic bond interactions between TB and SS. The adsorption capacities of TB on SS first increase and then decrease with the pH increasing from 3 to 9, and the optimal adsorption effect is achieved at pH = 6.0. The experimental studies show that SS has promising potential to act as an alternative adsorbent to remove cationic dyes from aqueous solutions.

AUTHOR INFORMATION

Corresponding Author

*Tel.: +86-535-6672176; fax: +86-535-6697667. E-mail address: unikguo@gmail.com (L. Guo).

Funding Sources

The authors acknowledge the National Natural Science Foundation of China (No. 21074050), the Natural Science Foundation of Shandong Province (ZR2010BM027), and the Scientific Research Award Foundation for Outstanding Young and Middle Aged Scientists of Shandong Province (BS2010CL012). The authors also greatly appreciate the support provided by the Project of Innovation Team Building of Ludong University (No. 08-CXB001).

REFERENCES

(1) National Bureau of Statistics of China, 2007. http://www.stats.gov.cn/tjsj/ndsj/2007/html/L1205e.htm.

(2) Lin, Y. H.; Leu, J. Y. Kinetics of Reactive Azo-Dye Decolorization by Pseudomonas Luteola in a Biological Activated Carbon Process. *Biochem. Eng. J.* **2008**, *39*, 457–467.

(3) Avlonitis, S. A.; Poulios, I.; Sotiriou, D.; Pappas, M.; Moutesidis, K. Simulated Cotton Dye Effluents Treatment and Reuse by Nanofiltration. *Desalination* **2008**, *221*, 259–267.

(4) Young, L.; Yu, J. Ligninase-Catalysed Decolorization of Synthetic Dyes. *Water Res.* **1997**, *31*, 1187–1193.

(5) Vlyssides, A. G.; Papaioannou, D.; Loizidoy, M.; Karlis, P. K.; Zorpas, A. A. Testing an Electrochemical Method for Treatment of Textile Dye Wastewater. *Waste Manage.* **2000**, *20*, 569–574.

(6) Sharma, Y. C.; Uma Optimization of Parameters for Adsorption of Methylene Blue on a Low-Cost Activated Carbon. *J. Chem. Eng. Data* **2010**, *55*, 435–439.

(7) Arami, M.; Limaee, N. Y.; Mahmoodi, N. M. Evaluation of the Adsorption Kinetics and Equilibrium for the Potential Removal of Acid Dyes Using a Biosorbent. *Chem. Eng. J.* **2008**, *139*, 2–10.

(8) Sharma, Y. C.; Uma; Sinha, A. S. K.; Upadhyay, S. N. Characterization and Adsorption Studies of Cocos nucifera L. Activated Carbon for the Removal of Methylene Blue from Aqueous Solutions. *J. Chem. Eng. Data* **2010**, *55*, 2662–2667.

(9) Hameed, B. H.; El-Khaiary, M. I. Batch Removal of Malachite Green from Aqueous Solutions by Adsorption on Oil Palm Trunk Fibre: Equilibrium Isotherms and Kinetic Studies. *J. Hazard. Mater.* **2008**, *154*, 237–244.

(10) Gupta, V. K.; Jain, R.; Shrivastava, M.; Nayak, A. Equilibrium and Thermodynamic Studies on the Adsorption of the Dye Tartrazine onto Waste "Coconut Husks" Carbon and Activated Carbon. *J. Chem. Eng. Data* **2010**, *55*, 5083–5090.

(11) Delval, F.; Crini, G.; Morin, N.; Vebrel, J.; Bertini, S.; Torri, G. The Sorption of Several Types of Dye on Crosslinked Polysaccharides Derivatives. *Dyes Pigm.* **2002**, *53*, 79–92.

(12) Crini, G. Recent Developments in Polysaccharide-based Materials Used as Adsorbents in Wastewater Treatment. *Prog. Polym. Sci.* **2005**, *30*, 38–70.

(13) Ozmen, E. Y.; Yilmaz, M. Use of β-cyclodextrin and Starch Based Polymers for Sorption of Congo Red from Aqueous Solutions. *J. Hazard. Mater.* **2007**, *148*, 303–310.

(14) Xu, S.; Wang, J.; Wu, R.; Wang, J.; Li, H. Adsorption Behaviors of Acid and Basic Dyes on Crosslinked Amphoteric Starch. *Chem. Eng. J.* **2006**, *117*, 161–167.

(15) Renault, F.; Morin-Crini, N.; Gimbert, F.; Badot, P. M.; Crini, G. Cationized Starch-based Material as a New Ion-exchanger Adsorbent for the Removal of C.I. Acid Blue 25 from Aqueous Solutions. *Bioresour. Technol.* **2008**, *99*, 7573–7586.

(16) Cui, D. P.; Liu, M. Z.; Liang, R.; Bi, Y. H. Synthesis and Optimization of the Reaction Conditions of Starch Sulfates in Aqueous Solution. *Starch/Stärke* **2007**, *59*, 91–98.

(17) Guo, L.; Li, G.; Liu, J.; Yin, P.; Li, Q. Adsorption of Aniline on Cross-Linked Starch Sulfate from Aqueous Solution. *Ind. Eng. Chem. Res.* **2009**, *48*, 10657–10663.

(18) Sheng, G. P.; Zhang, M. L.; Yu, H. Q. Characterization of Adsorption Properties of Extracellular Polymeric Substances (EPS) Extracted from Sludge. *Colloids Surf., B* **2008**, *62*, 83–90.

(19) Alpat, S. K.; Özbayrak, Ö.; Alpat, Ş.; Akçay, H. The Adsorption Kinetics and Removal of Cationic Dye, Toluidine Blue O, from Aqueous Solution with Turkish Zeolite. *J. Hazard. Mater.* **2008**, *151*, 213–220.
(20) Lagergren, S. About the Theory of So-called Adsorption of Soluble Substances. *K. Sven. Vetenskapsakad. Handl.* **1898**, *24*, 1–39.
(21) Ho, Y. S. *Adsorption of Heavy Metals from Waste Streams by Peat.* Ph.D. Thesis, University of Birmingham, Birmingham, U.K., 1995.
(22) Low, M. J. D. Kinetics of Chemisorption of Gases on Solids. *Chem. Rev.* **1960**, *60*, 267–312.
(23) Kumar, K. V. Linear and Non-Linear Regression Analysis for the Sorption Kinetics of Methylene Blue onto Activated Carbon. *J. Hazard. Mater. B* **2006**, *137*, 1538–1544.
(24) Kumar, K. V. Comparative Analysis of Linear and Non-Linear Method of Estimating the Sorption Isotherm Parameters for Malachite Green onto Activated Carbon. *J. Hazard. Mater.* **2006**, *136*, 197–202.
(25) Hameed, B. H.; El-Khaiary, M. I. Kinetics and Equilibrium Studies of Malachite Green Adsorption on Rice Straw-derived Char. *J. Hazard. Mater.* **2008**, *153*, 701–708.
(26) Langmuir, I. The Constitution and Fundamental Properties of Solids and Liquids. *J. Am. Chem. Soc.* **1916**, *38*, 2221–2295.
(27) Freundlich, H. M. F. Over the Adsorption in Solution. *Z. Phys. Chem.* **1906**, *57*, 385–470.
(28) Sips, R. On the Structure of a Catalyst Surface. *J. Chem. Phys.* **1948**, *16*, 490–495.
(29) Toth, J. State Equations of the Solid Gas Interface Layer. *Acta Chem. Acad. Sci. Hung.* **1971**, *69*, 311–317.
(30) Hisarli, G. The Effects of Acid and Alkali Modification on the Adsorption Performance of Fuller's earth for Basic Dye. *J. Colloid Interface Sci.* **2005**, *281*, 18–26.
(31) Talman, R. Y.; Atun, G. Effects of Cationic and Anionic Surfactants on the Adsorption of Toluidine Blue onto Fly Ash. *Colloids Surf., A* **2006**, *281*, 15–22.
(32) Hasany, S. M.; Chaudhary, M. H. Adsorption Behaviour of Microamounts of Cesium on Manganese Dioxide. *J. Radioanal. Nucl. Chem.* **1984**, *84*, 247–256.
(33) Saleem, M.; Afzal, M.; Qadeer, R.; Hanif, J. Selective Adsorption of Uranium on Activated Charcoal from Electrolytic Solutions. *Sep. Sci. Technol.* **1992**, *27*, 239–253.
(34) Şener, S. Use of Solid Wastes of the Soda Ash Plant as an Adsorbent for the Removal of Anionic Dyes: Equilibrium and Kinetic Studies. *Chem. Eng. J.* **2008**, *138*, 207–214.
(35) Demir, H.; Top, A.; Balköse, D.; Ülkü, S. Dye Adsorption Behavior of Luffa Cylindrica Fibers. *J. Hazard. Mater.* **2008**, *153*, 389–394.
(36) Bekci, Z.; Seki, Y.; Yurdakoc, M. K. Equilibrium Studies for Trimethoprim Adsorption on Montmorillonite KSF. *J. Hazard. Mater.* **2006**, *133*, 233–242.
(37) Wang, J.; Somasundaran, P. Study of Galactomannose Interaction with Solids Using AFM, IR and Allied Techniques. *J. Colloid Interface Sci.* **2007**, *309*, 373–383.
(38) Panneer Selvam, P.; Preethi, S.; Basakaralingam, P.; Thinakaran, N.; Sivasamy, A.; Sivanesan, S. Removal of Rhodamine B from Aqueous Solution by Adsorption onto Sodium Montmorillonite. *J. Hazard. Mater.* **2008**, *155*, 39–44.
(39) Rauf, M. A.; Qadri, S. M.; Ashraf, S.; Al-Mansoori, K. M. Adsorption Studies of Toluidine Blue from Aqueous Solutions onto Gypsum. *Chem. Eng. J.* **2009**, *150*, 90–95.
(40) van de Ven, T. G. M.; Saint-Cyr, K.; Allix, M. Adsorption of Toluidine Blue on Pulp Fibers. *Colloids Surf., A* **2007**, *294*, 1–7.